JEE Journal of Ecological Engineering

Journal of Ecological Engineering 2022, 23(10), 98–106
https://doi.org/10.12911/22998993/152363
ISSN 2299-8993, License CC-BY 4.0

Received: 2022.07.11
Accepted: 2022.08.12
Published: 2022.09.01

Development of Fiber-Optic Sensors System, Based on Fiber Bragg Gratings

Aliya Kalizhanova[1], Murat Kunelbayev[1], Waldemar Wojcik[2], Ainur Kozbakova[1], Zhalau Aitkulov[3], Feruza Malikova[1]

[1] Institute of Information and Computational Technologies, Al-Farabi Kazakh National University, Al-Farabi Avenue 71, Almaty, 50040, Kazakhstan

[2] Lublin University of Technologies, ul. Nadbystrzycka 40, 20-618 Lublin, Poland

[3] Institute of Information and Computational Technologies, Academic of Logistic and Transport, Shevchenko St., 97, Almaty, Kazakhstan

* Corresponding author's e-mail: kalizhanova_aliya@mail.ru

ABSTRACT

An article herein considers the development of a fiber-optic sensor system, based on fiber Bragg gratings. Presently, fiber-optic sensors has become world-widely known amongst sensor technologies, used for monitoring engineering and construction structures. The work is linked with developing the system from fiber-optic sensors on the basis of fiber optic gratings, its characteristics, deformation behavior and temperature, acting at fiber Bragg grating by means of computer modeling. The research is focused at the analysis of characteristics and deformation and temperature behavior of fiber-optic Bragg sensor. Fiber-optic Bragg sensor with tilted grating is used for measuring deformation of the object, the strength of which is changed, dependent on the applied force, as well, for measuring and detecting any temperature deviations, influencing at fiber Bragg grating, which might bring to fire and accidents. In the research, simulation modeling there was made in the MATLAB (Simulink) software.

Keywords: fiber Bragg grating, sensors, deformation, temperature, modeling, MATLAB (Simulink).

INTRODUCTION

Fiber-optic sensors are widely used for measuring deformation and temperature of composite materials, thanks to sufficient advantages: small diameter (less, than 150 mm), small weight, corrosion resistance. FBG sensor has reflective index modulation along the length of a single-mode optical fiber. Figure 1(a) shows chart of FBG sensor, which consists of the core, cladding and coating. Light travels in the core due to full internal reflection on the border of the core and cladding. Optical fiber is usually covered with coating (for instance, polyimide) to protect the fiber surface and lessen the strain concentration around built-in fiber [Takeda 2005,Takeda 2014]. When floodlight is in FBG sensor, the narrow spectral subcomponent is reflected inversely from the grating area (Fig. 1b).

Figure 2a, 2b shows a schematic diagram of FBG sensor, enclosed into capillary pipe and sealed from both edges, using rapid-curing araldite [Boateng 2019].

The sensors with fiber Bragg grating, widely used for control over the health of composite structures in civil, airspace and wing-energy industries in the works [Minakuchi 2013, Takagaki 2017, Her 2017, Umer 2012, Moriche 2016, Böger 2008, Giri 2015]. Strain-measuring sensors to control deformation, which secure short precision due to their reference dimension with regard to reinforcing fibers in the article [Moriche 2016] there was developed. FBG sensors offer the solution, which does not allow laminated structure breakdown (usually with a diameter of 125–300 micron), they are inert and sensitive to both temperature and mechanical loading. In the works [Chiang 2011, Antonucci 2006,

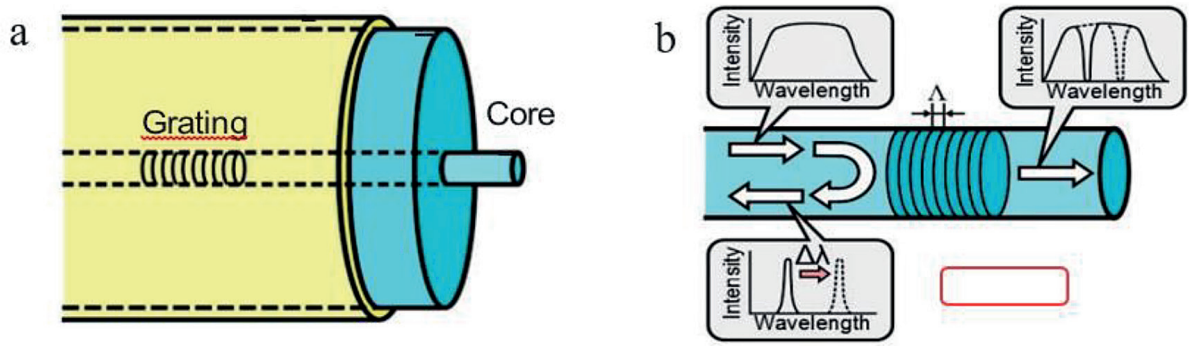

Figure 1. FBG sensor chart: a) total construction and b) FBG core with measuring principle [Takeda 2005, Takeda 2014]

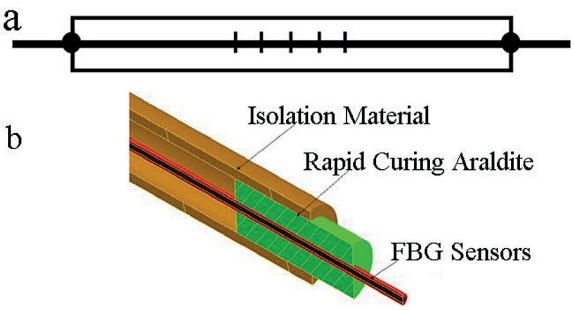

Figure 2. a) Chart of FBG sensor, enclosed into a tube with fastened both edges, b) view of isolation material cross-section with FBG sensor [Boateng 2019]

Murukeshan 2000], FBG technologies there were used to monitor thermoactive resin curing for airspace and wing energy industries.

The optoelectronic sensor system, shown in Figure 3, which consisted of two light sources: superluminescent diode for lighting Bragg grating sensor and laser diode with 1310 Nm wavelength to light the fiber edge in the article [Antonucci 2006] there was developed.

Figure 4 shows the interrogation system with grating [Murukeshan 2000], used for research. Light from light-emitting diode unites with optical fiber, which is broken down into two by means of fiber coupler 2/2. Interrogating brancher arm 2/2 is equipped with nuclear FBG with certain wavelength selection. Reflected wavelength is studied, using picowave reference system, as it is shown in the Figure. Most researchers mentioned in the article herein are conducted, using this system configuration, except the devices for various tests. Interrogation system with Bragg grating was used by Micron-optics company for interrogating inverse signals. Collecting, processing and imaging the data were fulfilled, using National Instrument PC-DIO-24DAQ card.

Regardless of big executed work on characterization of FBG sensors for monitoring systems state, only several researches informed about successful usage of FBG sensors at high temperatures, low deformation, as well, at resin curing or gel formation at the moment / time. There exists a lot of techniques for treat monitoring in

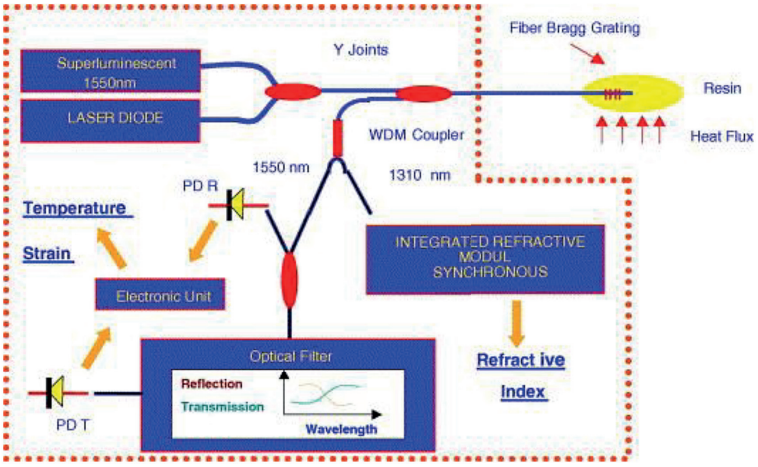

Figure 3. Optoelectronic sensor system [12]

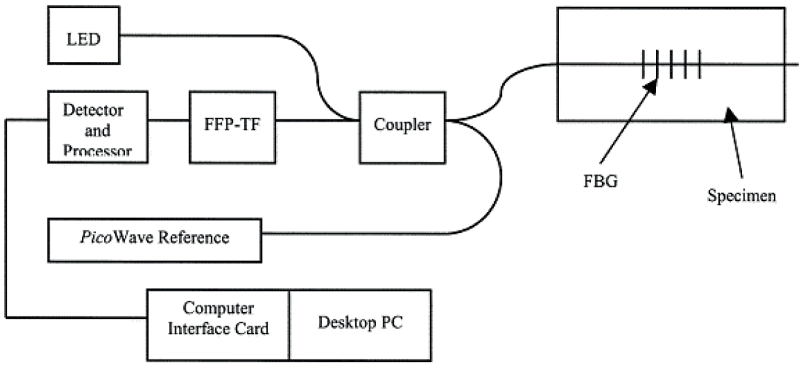

Figure 4. Interrogation system with Bragg grating [Murukeshan 2000]

autonomous regime, but only few on-line methods are accessible [Grattan 2000, Hill 1997, Mahendran 2009, Koissin 2014, Minakuchi 2016, Anil Kumar 2016, Hu 2017, Umer 2015, Gagné 2014, De Lima Filho 2014].

To characterize FBG, the authors used passive system of temperature decontaminating, which permits slow heat exchange with two temperature baths, laboratory air and liquid nitrogen (LN2) [De Lima Filho 2014]. Scheme of experimental installation is given in Figure 5.

Figure 6 shows the basic diagram of Bragg wavelength interrogator with wideband signal (BIBS) and FBG [De Lima Filho 2014]. FBG reflection spectra are measured with an optical spectrum analyzer ANDO AQ6317B (OSA), switched on to the third port of optical circulator, the first port of which is powered from the wideband source of C-range (BBS) of model BBS 1560 + 2FA00 from JDS Uniphase. Optical circulator transfers power from the first to the second port, to which the FBG is switched on. Reflection capacity from FBG entered the second port and went to the third port.

Figure 7 shows computing logical schemes for model Simulink [Boateng 2019]. By means of

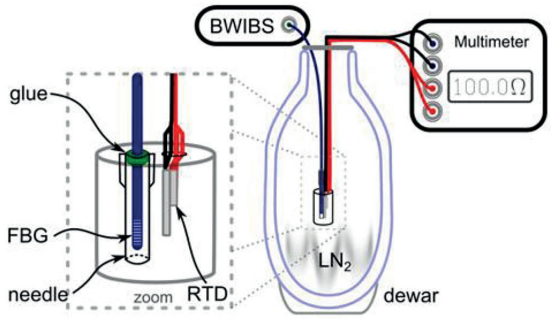

Fig. 5. Diagram of a temperature control microchamber [23]

Matlab Simulink logical diagrams, there Simulink model was shown, solved at various temperatures. Models of MATLAB/Simulink logical block for uncoated and coated FBG, enclosed into a capillary tube, are shown in Figure 7, accordingly.

Figure 8 shows modeling of three models logical schemes, constructed using logical diagrams where forces, deformations and temperatures in units can be computed [Schubela 2018].

In the article herein, the system from fiber-optic sensors, based on fiber Bragg gratings there is presented, which is focused at digital theoretical demonstration and modeling the fiber Bragg grating, using MATLAB (Simulink), which give effects of fiber Bragg grating.

MATERIALS AND METHODS

Modeling the computer program MATLAB (Simulink), used for designing the system of fiber-optic sensors, based on fiber Bragg gratings, parameters are set for fiber Bragg grating, used in modeling herein, to measure deformation and temperature of fiber Bragg grating with Bragg wavelength displacement and spectral reflection ability for both reflection indices and grating length.

Theoretically normalized reflection is created with fiber Bragg grating. Reflected wavelength λ, called Bragg wavelength, is clarified in the correlation herein:

$$\lambda_B = 2ne\Lambda \tag{1}$$

Wavelength changes in fiber Bragg grating due to temperature and deformation can be linked with the following equation:

$$\Delta\lambda_B = \lambda_B(1 - \rho_e)\varepsilon \tag{2}$$

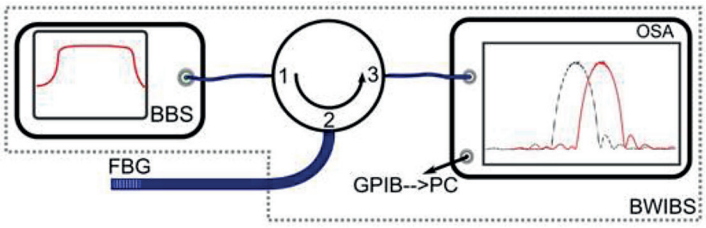

Figure 6. Schematic diagram of the Bragg wavelength interrogator with broadband signal (BWIBS) and FBG [23]

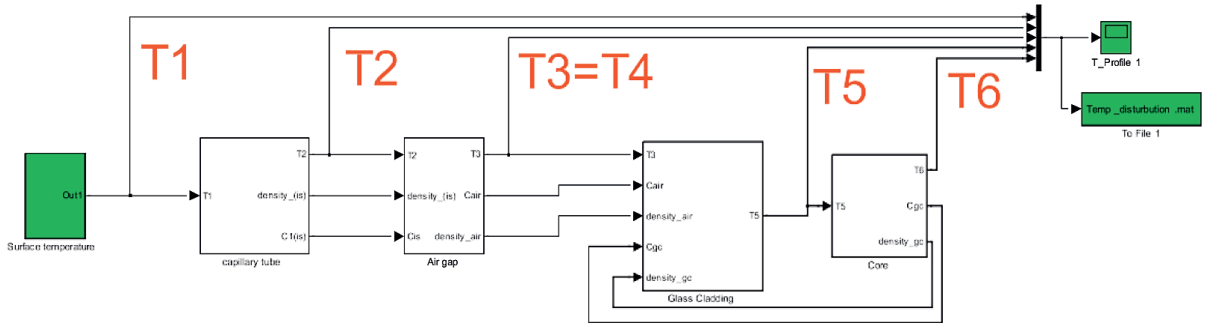

Figure 7. Computing logical schemes for Simulink model [Boateng 2019]

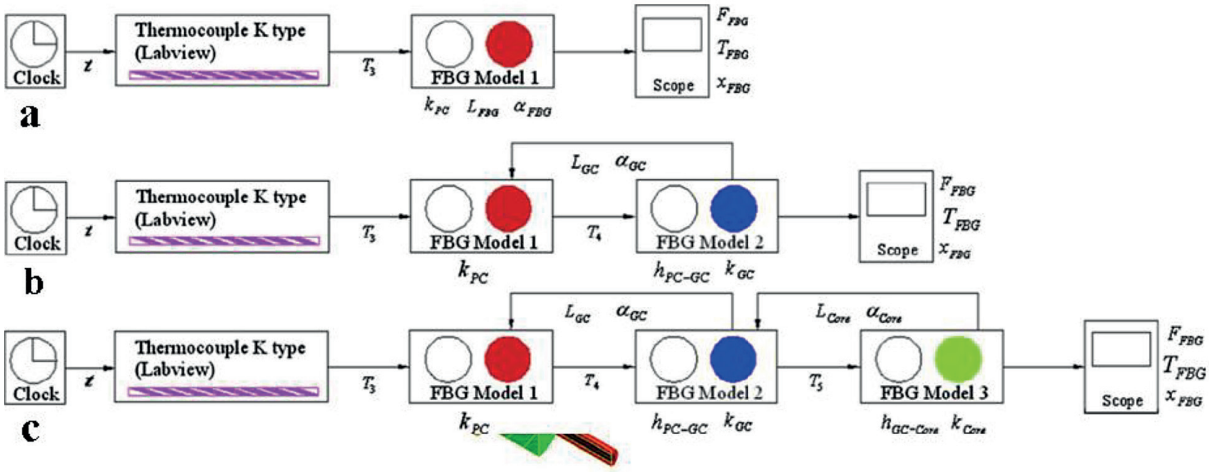

Figure 8. Logic diagram of three models: (a) First model, (b) Second model, (c) Third model [Schubela 2018]

Amplitude reflection spectrum of uniform fiber Bragg grating is defined with a following equations:

$$R(L,\lambda) = \frac{K^2 sinh^2(\gamma L)}{\Delta\beta^2 sinh^2 + k^2 cosh^2(\gamma L)} \quad (3)$$

$$R(L,\lambda) = \tanh^2(\gamma L) \quad (4)$$

RESULTS AND DISCUSSION

To model the system from fiber-optic sensors, based on fiber Bragg gratings, it is necessary to demonstrate features and behavior of fiber Bragg grating. Bragg wavelength displacement changes are due to strain and temperature. Spectral reflection ability of fiber sensors with Bragg grating changes at different variation of reflection index and grating length.

Figure 9 shows the system of fiber-optic sensors, based on fiber Bragg gratings. The system consists of source unit in Simulink, which is modeled as a source of Transfer Matrix Method 1550 Nm central wavelength and in 1540–1550 Nm range. That source is set going to FBG through filter. The filter restricts only a narrow band, which shall be sent to FBG sensor. From every FBG with central wavelength in the area of ultraviolet excimer laser it is reflected back, dependent on reflective spectra of separate FBG.

Figure 10 shows increase of dependence of deformation on Bragg wavelength. As it is seen from the given Figure, the deformation is increased along with fiber wavelength. Fiber wavelength changes, comparing to its initial wavelength, in which the fiber detects deformation.

Figure 11 shows increase of the dependence of temperature on Bragg wavelength displacement. As it is seen from the Figure, Bragg wavelength displacement shows increase, if temperature changes higher up. Bragg wavelength displacement was measured at temperature rise. Temperature change increased up to 220°C, while Bragg wavelength displacement continues to increase up to 11,59456.

Figure 12 shows spectrum of fiber Bragg grating reflection with different change of reflective index at grating length L = 1 mm. As it is seen from the Figure, reflection capacity of fiber Bragg grating alters at different changes of reflective index. Spectral reflection capacity increases along with increasing of reflective index change. It increases up to 70% at Δn = 0.007, when grating length was 0.5 mm.

Figure 13 shows change spectrum of fiber Bragg grating reflection with different grating length at reflective index change Δn = 0.0003. As it is seen from the Figure 14, changes of spectral reflection capacity vary at different grating length 0.5 mm, and reflective index changes were fixed at Δn = 0.0001. Reflection capacity was observed

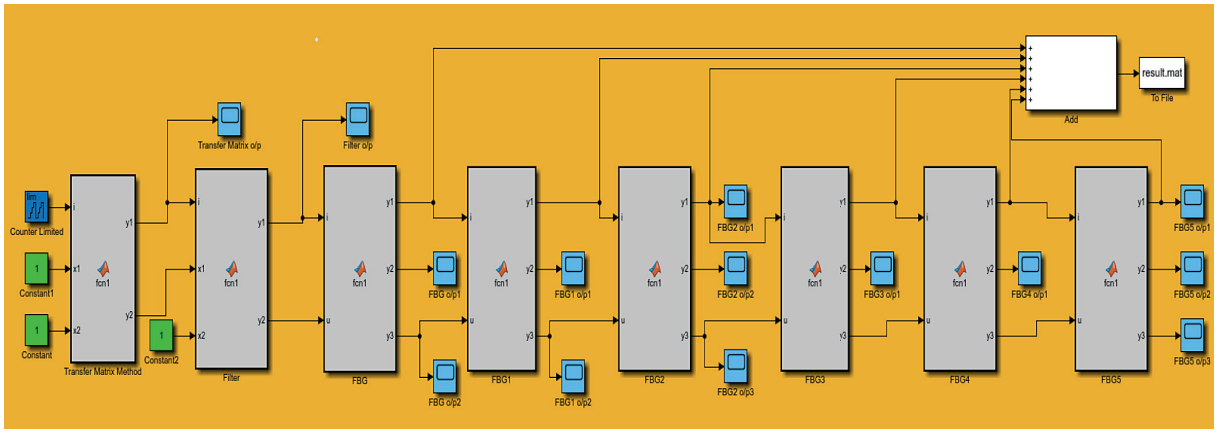

Figure 9. Systems from fiber-optic sensors, based on fiber Bragg gratings

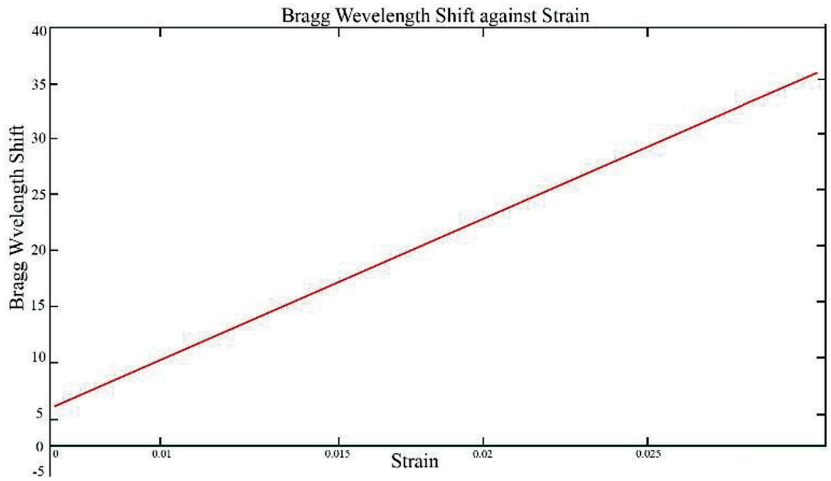

Figure 10. Dependence of deformation on Bragg wavelength

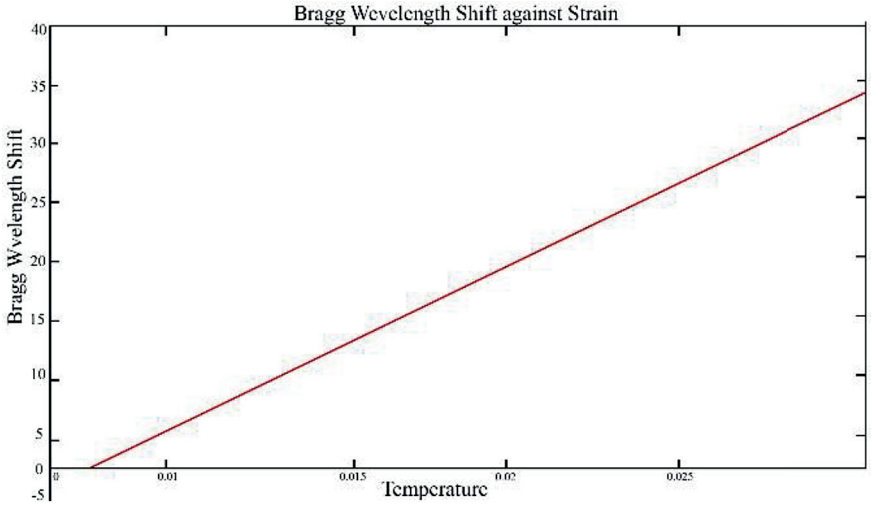

Figure 11. Dependence of temperature on Bragg wavelength displacement

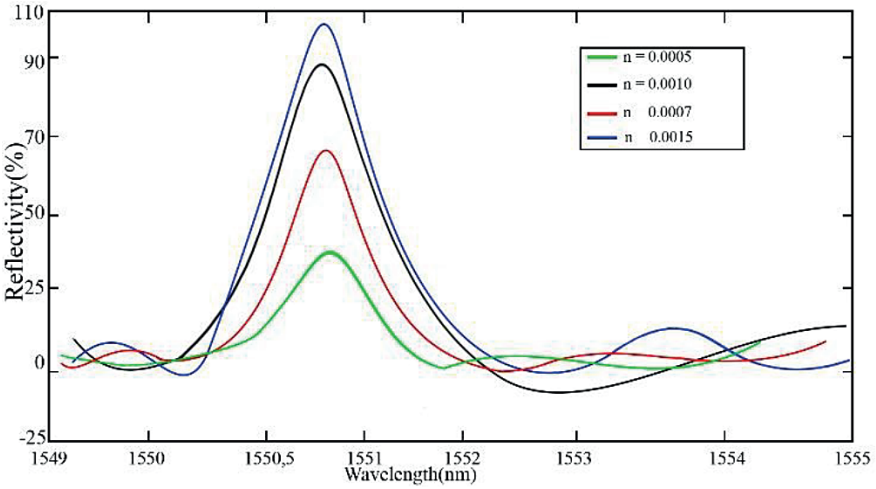

Figure 12. Spectrum of fiber Bragg grating reflection with different change of refractive index at grating length L = 0.5 mm

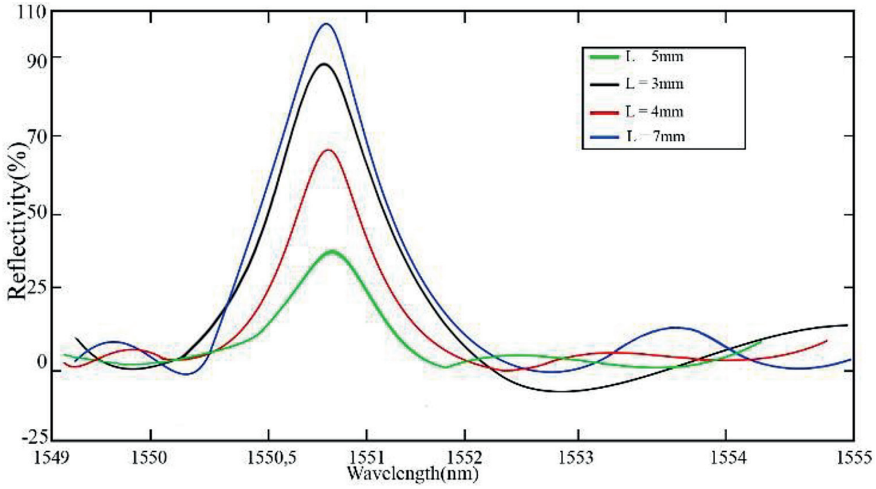

Figure 13. Spectrum of fiber Bragg grating reflection with different grating length at reflective index change Δn = 0.0001

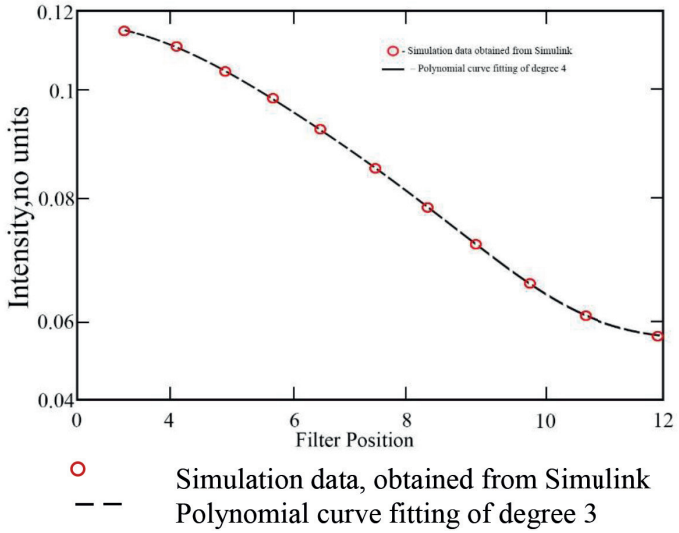

Figure 14. Reflective spectra from fiber sensors network with 4 FBG, dependent on filter position

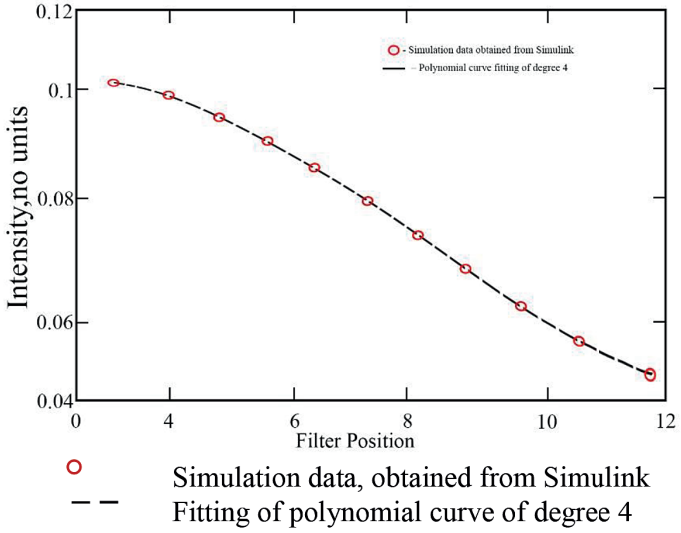

Figure 15. Reflection spectra from fiber sensor network with 5 FBG, dependent on filter position

with grating length increase. While grating length increases up to 1 mm, the spectral reflection capacity grows up to 70%, when change of reflective index was set as constant at $\Delta n = 0.0001$.

As it is seen from the picture, the sum of laser reflection capacity from 4 FBG was measured in spectrum analyzer, which represents output intensity, which will be measured at interrogation device, where the filter is with 0.01 Nm pitch. Root-mean-square error (RMSE) for polynomial fitting of 4th degree is 4.250×10^{-4}.

Figure 15 shows at reflection spectra from fiber sensor network with 5 FBG dependent on filter position. As it is seen from the Figure, using 5 FBG, the data complies with polynomial of 5th degree, with RMSE: 5.675×10^{-4}.

CONCLUSIONS

The presented herein offered to develop the system from fiber-optic sensors, based on fiber Bragg gratings by means of MATLAB (Simulink). It was designed for developing the code and modeling fiber-optic sensor, based on fiber Bragg gratings. There was computed deformation, temperature and spectral reflection capacity both for different reflective index change and grating length. At simulation it is seen that deformation occurs when fiber length changes, comparing to its initial length. Deformation rises along with Bragg wavelength displacement increase, and temperature has linear distribution. Bragg wavelength displacement actually

influences at temperature, when Bragg wavelength displacement increases, temperature, as well, rises. Also, it was computed that the sum of laser reflected power from 4 FBG was measured in spectrum analyser, which represents the output intensity, which will be measured at interrogation device, where the filter is with 0.01 Nm pitch. Root-mean-square error (RMSE) for fitting polynomial of degree 4 is 4.250×10^{-4}, and, at using 5 FBG the data complies with degree 5, with RMSE: 5.675×10^{-4}. As it is seen from the research presented herein, the system from fiber-optic sensors, based on fiber Bragg gratings, consisting of five fiber-optic sensors operates in full mode and offers good results.

Acknowledgments

This work is supported by grant from the Ministry of Education and Science of the Republic of Kazakhstan within the framework of the Project No. AP09259547 "Development of a system of distributed fiber-optic sensors based on fiber Bragg gratings for monitoring the state of building structures", Institute Information and Computational Technologies CS MES RK. Experimental researches have been carried out in the laboratories of optoelectronics at the Electric engineering and computer sciences faculty of Lublin Technical University.

REFERENCES

1. Takeda N., Okabe Y., Kuwahara J., et al. 2005. Development of smart composite structures with small-diameter fiber Bragg grating sensors for damage detection: Quantitative evaluation of delamination length in CFRP laminates using Lamb wave sensing. Compos Sci Technol, 65, 2575–2587.
2. Takeda S., Tsukada T., Sugimoto S., et al. 2014. Monitoring of water absorption in CFRP laminates using embedded fiber Bragg grating sensors. Compos Part A Appl Sci Manuf, 61, 163–171.
3. Boateng E., Schubel P., Umer R. 2019. Thermal isolation of FBG optical fibre sensors for composite cure monitoring. Sensors and Actuators A, 287, 158–167.
4. Minakuchi S., Takeda N. 2013. Recent advancement in optical fiber sensing for aerospace composite structures. Photonic Sens, 3(4), 345–354.
5. Takagaki K., Hisada S., Minakuchi S., Takeda N. 2017.Process improvement for out-of- autoclave prepreg curing supported by in-situ strain monitoring. J Compos Mater, 51(9), 1225–1237.
6. Her S.-C., Huang C.-Y. 2013. Thermal strain analysis of optic fiber sensors. Sensors, 13, 1846–1855.
7. Umer R., Waggy E.M., Haq M., Loos A.C. 2012. Experimental and numerical characterizations of flexural behavior of VARTM-infused composite sandwich structures. J Reinf Plast Compos, 31(2), 67–76.
8. Moriche R., Sánchez M., Jiménez-Suárez A., Prolongo S.G., Ureña A. 2016. Strain monitoring mechanisms of sensors based on the addition of graphene nanoplatelets into an epoxy matrix. Compos Sci Technol, 123 (Suppl. C), 65–70.
9. Böger L., Wichmann M.H.G, Meyer L.O., Schulte K. 2008. Load and health monitoring in glass fibre reinforced composites with an electrically conductive nanocomposite epoxy matrix. Compos Sci Technol, 68(7), 1886–1894.
10. Giri A., Pandey C., Mahapatra M.M., Sharma K., Singh P.K. 2015. On the estimation of error in measuring the residual stress by strain gauge rosette. Measurement, 65, 41–92.
11. Chiang C.-C. 2011.Curing monitoring of composite material using embedded fiber Bragg grating sensors. In: Těšinova P (Ed.) Advances in composite materials – analysis of natural and man-made materials, In Tech, 345–360.
12. Antonucci V., et al. 2006. Real time monitoring of cure and gelification of a thermoset matrix. Compos Sci Technol, 66(16), 3273–3280.
13. Murukeshan V.M., et al. 2000.Cure monitoring of smart composites using Fiber Bragg Grating based embedded sensors. Sens Actuators A, 79(2), 153–161.
14. Grattan K.T.V., Sun D.T. 2000.Fiber optic sensor technology: an overview. Sens Actuators, 82(1–3), 40–61.
15. Hill K.O., Meltz G. 1997. Fiber Bragg grating technology fundamentals and overview. J Lightwave Technol, 15(8), 1263–1276.
16. Mahendran R.S., et al. 2009. Fiber-optic sensor design for chemical process and environ- mental monitoring. Opt Lasers Eng, 47(10), 1069–1076.
17. Koissin V., Demčenko A., Korneev V.A. 2014. Isothermal epoxy-cure monitoring using nonlinear ultrasonics. Int J Adhesion Adhesiv, 52(Suppl. C), 11–18.
18. Minakuchi S., Niwa S., Takagaki K., Takeda N. 2016. Composite cure simulation scheme fully integrating internal strain measurement. Compos A Appl Sci Manuf, 84, 53–63.
19. Anil Kumar A., Sundaram R. 2016.Cure cycle optimization for the resin infusion technique using carbon nanotube additives. Carbon, 96 (Suppl. C), 1043–1052.

20. Hu H., Li S., Wang J., Zu L., Cao D., Zhong Y. 2017. Monitoring the gelation and effective chemical shrinkage of composite curing process with a novel FBG approach. Compos Struct, 176 (Suppl. C), 187–194.
21. Umer R., Li Y., Dong Y., Haroosh H.J., Liao K. 2015. The effect of graphene oxide (GO) nanoparticles on the processing of epoxy/glass fiber composites using resin infusion. Int J Adv Manuf Technol, 81(9), 2183–2192.
22. Gagné M., Loranger S., Lapointe J., Kashyap R. 2014. Fabrication of high quality, ultra-long fiber Bragg gratings: up to 2 million periods in phase. Opt. Exp, 22, 387–398.
23. De Lima Filho E.S., Diaa Baiad M., Gagné M., Kashyap R. 2014. Fiber Bragg gratings for low- temperature measurement. Opt. Exp, 22, 27681–27694.
24. Boateng E., Schubel P., Umer R. 2019.Thermal isolation of FBG optical fibre sensors for composite cure monitoring Sensors and Actuators A, 287, 158–167.
25. Schubela P., Umera R., Boateng E. 2018. Modelling heat transfer through an FBG optical fibre. Composites Part A: Applied Science and Manufacturing, 109, 184–196.